

Chirped-quasi-periodic structure for quasi-phase-matching

J. Yang,^{1,*} X. P. Hu,^{1,2} P. Xu,¹ X. J. Lv,¹ C. Zhang,¹ G. Zhao,¹ H. J. Zhou,¹ and S. N. Zhu^{1,3}

¹National Laboratory of Solid State Microstructures and Department of Physics, Nanjing University, Nanjing 210093, China

²xphu@nju.edu.cn

³zhushn@nju.edu.cn

*wyajy@gmail.com

Abstract: We propose in this paper a chirped-quasi-periodic structure using the projection method. This type of new structure combines the advantages of chirped and quasi-periodic structures, and can be used for both multiple quasi-phase-matching and multiple bandwidths control. Numerical simulation of second-harmonic generation performance is in good agreement with the Fourier spectrum of the structure.

©2010 Optical Society of America

OCIS codes: (130.7405) Wavelength conversion devices; (190.4410) Nonlinear optics, parametric processes.

References and links

1. S. N. Zhu, Y. Y. Zhu, and N. B. Ming, "Quasi-phase-matched third-harmonic generation in a quasi-periodic optical superlattice," *Science* **278**(5339), 843–846 (1997).
2. C. Zhang, H. Wei, Y. Y. Zhu, H. T. Wang, S. N. Zhu, and N. B. Ming, "Third-harmonic generation in a general two-component quasi-periodic optical superlattice," *Opt. Lett.* **26**(12), 899–901 (2001).
3. B. Y. Gu, B. Z. Dong, Y. Zhang, and G. Z. Yang, "Enhanced harmonic generation in aperiodic optical superlattices," *Appl. Phys. Lett.* **75**(15), 2175–2177 (1999).
4. A. H. Norton, and C. M. de Sterke, "Aperiodic 1-dimensional structures for quasi-phase matching," *Opt. Express* **12**(5), 841–846 (2004).
5. Z. W. Liu, Y. Du, J. Liao, S. N. Zhu, Y. Y. Zhu, Y. Q. Qin, H. T. Wang, J. L. He, C. Zhang, and N. B. Ming, "Engineering of a dual-periodic optical superlattice used in a coupled optical parametric interaction," *J. Opt. Soc. Am. B* **19**(7), 1676–1684 (2002).
6. M. Asobe, O. Tadanaga, H. Miyazawa, Y. Nishida, and H. Suzuki, "Multiple quasi-phase-matched LiNbO₃ wavelength converter with a continuously phase-modulated domain structure," *Opt. Lett.* **28**(7), 558–560 (2003).
7. X. P. Hu, G. Zhao, C. Zhang, Z. D. Xie, J. L. He, and S. N. Zhu, "High-power, blue-light generation in a dual-structure, periodically poled, stoichiometric LiTaO₃ crystal," *Appl. Phys. B* **87**(1), 91–94 (2007).
8. Z. D. Gao, S. N. Zhu, S.-Y. Tu, and A. H. Kung, "Monolithic red-green-blue laser light source based on cascaded wavelength conversion in periodically poled stoichiometric lithium tantalate," *Appl. Phys. Lett.* **89**(18), 181101 (2006).
9. G. K. Samanta, and M. Ebrahim-Zadeh, "Continuous-wave, single-frequency, solid-state blue source for the 425–489 nm spectral range," *Opt. Lett.* **33**(11), 1228–1230 (2008).
10. M. A. Arbore, O. Marco, and M. M. Fejer, "Pulse compression during second-harmonic generation in aperiodic quasi-phase-matching gratings," *Opt. Lett.* **22**(12), 865–867 (1997).
11. G. Imeshev, "Tailoring of Ultrafast Frequency Conversion with Quasi-Phase-Matching Gratings," Ph.D. dissertation (Stanford University, 2000).
12. X. J. Lv, Z. Sui, Z. D. Gao, M. Z. Li, Q. H. Deng, and S. N. Zhu, "Bandwidth and stability enhancement of optical parametric amplification using chirped ferroelectric superlattice," *Opt. Laser Technol.* **40**(1), 21–29 (2008).
13. R. K. P. Zia, and W. J. Dallas, "A simple derivation of quasi-crystalline spectra," *J. Phys. Math. Gen.* **18**(7), L341–L345 (1985).
14. A. Yariv, and P. Yeh, *Optical Waves in Crystal* (Wiley, 1984).

1. Introduction

One of the challenges in the field of nonlinear frequency conversion is to design a single poled grating structure that can simultaneously quasi-phase-match several different $\chi^{(2)}$ processes [1–6]. A $\chi^{(2)}$ process involves the nonlinear mixing of two waves to produce a third wave at the sum or difference frequency. The process proceeds efficiently if the quasi-phase-

matching (QPM) condition is satisfied. For example, in a sum frequency generation process $\omega_1 + \omega_2 = \omega_3$, the QPM condition requires the wave vector mismatch between three waves $\Delta k = k_3 - k_2 - k_1$ be compensated by a reciprocal lattice vector G , i.e. $G = k_3 - k_2 - k_1$.

If a single $\chi^{(2)}$ process is desired, it is well known that for obtaining the largest Fourier coefficient the grating need to be periodically poled with period $\Lambda = 2\pi / G$. If several $\chi^{(2)}$ processes are desired to be cascaded into one grating, the structure of the grating needs to be fabricated by some new means, such as quasi-periodic structures [1,2], aperiodic structures [3,4], dual-periodic structures [5], numerically optimized phase modulation [6] and so forth.

However, in cascaded $\chi^{(2)}$ processes, for effective generation of every process the matching temperatures of all these processes need to be the same. For example, in a third-harmonic generation (THG) process [1], the third-harmonic (TH) wave is achieved by two steps—a second harmonic generation (SHG) cascading a sum frequency generation (SFG). Theoretically, using Sellmeier equation of the nonlinear material we can design a structure to quasi-phase-match these two processes perfectly. Practically, however, the QPM condition is sensitive. Tiny inaccuracy of Sellmeier equation or slight error of domain period will cause great shifts of the matching temperature of these processes. Therefore, the two bandwidths will not overlap well for efficient THG [7]. Moreover, for other cascaded processes such as an optical parametric oscillation (OPO) cascading a SFG or SHG [8,9], bandwidth matching of the two cascading processes is a crucial factor for generating desired visible light effectively.

As is known, chirped structure [10–12] can be used to broaden acceptance bandwidth in nonlinear optical interactions. To solve the problem mentioned above, here we propose a novel structure for both multiple QPM and bandwidths controlling. The key point of our idea is to introduce chirping into quasi-periodic structure to design a chirped-quasi-periodic (CQP) structure. This idea provides more flexibility for structure designing of QPM gratings.

The paper is organized as follows: In Section 2, the designing approach of CQP structure is derived using projection method. A concrete CQP structure is analyzed in Fourier space in Section 3. Numerical simulations using SHG to verify the validity of the structure are given in Section 4. And in Section 5 is our conclusion.

2. Structure design

A one-dimensional quasi-periodic (QP) structure can be obtained by projection from a square lattice [13], in which the ‘hidden symmetry’ of the one-dimensional QP structure is displayed. See Fig. 1. The projection line ζ has an angle θ to x axis. We label the orthogonal line to ζ as η axis and let the width of the projection window equal to the sum of the projection from unit spacing of x and y axis to η axis, i.e. $w = \sin\theta + \cos\theta$, as shown in Fig. 1. As long as the projection angle θ is irrational, the arrangement of the structure will be quasi-periodic.

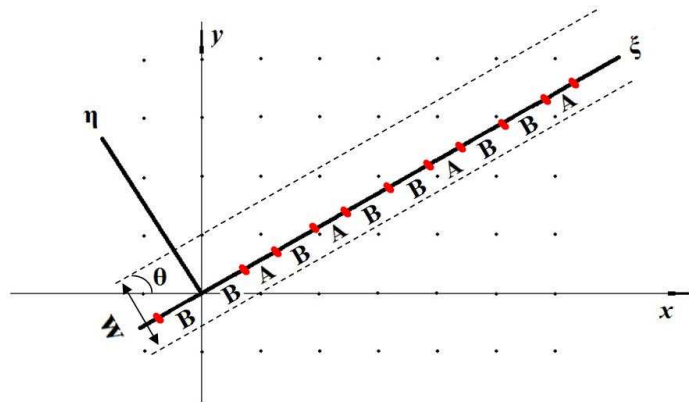


Fig. 1. Schema of the projection method to obtain a quasi-periodic structure.

From the projection method described above, we can obtain a two-component quasi-periodic structure. The two components—block *A* and block *B*—are projected by vertical and horizontal spacing, respectively. For dielectric optical superlattice such as periodically-poled lithium niobate (PPLN) or lithium tantalite (PPLT), we set both block *A* and *B* consisting of a positive domain and a negative domain, and the lengths of the positive domains in each block have the same value *l*. The reciprocal vectors of this structure are given in Ref [2]:

$$G_{m,n} = 2\pi \frac{m + n\tau}{\tau D_A + D_B}, \quad (1)$$

where the arrangement parameter τ is equal to the proportion of block number of *A*, N_A , to block number of *B*, N_B , i.e. $\tau = N_A / N_B$. D_A, D_B are the lengths of block *A* and *B*, respectively.

When the quasi-periodic arrangement is projected from a square lattice, the proportion D_A / D_B is fixed, and we have $\tau = \tan\theta$. However, in a more general situation, D_A / D_B is an adjustable parameter [2]. Under such circumstance the quasi-periodic arrangement needs to be projected from a rectangular lattice instead, and τ still indicates the proportion of block numbers, but the relation $\tau = \tan\theta$ do not hold any more.

Considering the situation of a rectangular lattice, let d_x and d_y indicate the horizontal and the vertical spacing, respectively. Then we can obtain the expression of τ :

$$\tau = \frac{N_A}{N_B} = \frac{d_x}{d_y} \tan \theta. \quad (2)$$

Equation (2) indicates the arrangement parameter τ varies with the spacing of the projection lattice.

We present here a new grating designing approach which introduces the chirping factor into QP grating. Specifically, in the projection method described above, if we chirp the spacing of the original projection lattice first, then the influence of chirping will be hidden in the projected quasi-periodic structure, so that we obtain a chirped-quasi-periodic structure. To obtain a CQP structure we could chirp its horizontal and/or vertical spacing.

For a linear chirping, we can define a chirp factor *r* to describe the chirp rate, see Ref [3]:

$$r_{x(y)} = \frac{d_{x(y)}(N) - d_{x(y)}(1)}{d_{x0(y0)}}, \quad (3)$$

where $d_i(1)$, $d_i(N)$ and d_{i0} represent the length of the first, the last and the nominal spacing of the lattice, $i = x, y$ indicates horizontal and vertical, respectively. The *n*th spacing's length is:

$$d_{x(y)}(n) = d_{x(y)}(1) + \frac{n}{N} r_{x(y)} d_{x0(y0)}. \quad (4)$$

However, chirping is not limited to linear [11]. Indeed, as long as the domain period varies with position, linearly or non-linearly, the grating can be considered as chirped.

Here we present the general situation. We set both spacing vary with position arbitrarily, i.e. $d_x = d_x(\zeta)$ and $d_y = d_y(\zeta)$, ζ is the coordinate along the direction of the QP grating. From Fig. 1 we can see that using variable ζ to describe the spacing variation is equivalent to using coordinate *x* and *y* since they are proportional. Moreover, here we use continuous functions to describe discrete spacing, which is the same as Eq. (4) in Ref.12. Actually, for a given starting point, using a recursion method the desired structure can be easily obtained.

Generally, introducing of chirping will bring two kinds of influences to the QP structure. First, chirping the projection lattice will apparently affect the length of the blocks. Since all blocks *A* are projected from vertical spacing while all blocks *B* are projected from horizontal spacing, the block lengths D_A and D_B will vary with position ζ as following forms:

$$D_A(\xi) = d_y(\xi) \sin \theta, \quad (5)$$

$$D_B(\xi) = d_x(\xi) \cos \theta. \quad (6)$$

Secondly, chirping will also affect the arrangement parameter τ . From Eq. (2) we know that for a CQP structure τ can be expressed as:

$$\tau(\xi) = \frac{d_x(\xi)}{d_y(\xi)} \tan \theta. \quad (7)$$

Noticing that τ is a localized parameter in a CQP structure, different positions ξ have different quasi-periodic arrangements, which is totally different from the traditional QP structure. Substituting Eq. (5-7) into the expression of reciprocal vectors Eq. (1), we obtain:

$$G_{m,n}(\xi) = 2\pi \left(\frac{m \cos \theta}{d_x(\xi)} + \frac{n \sin \theta}{d_y(\xi)} \right) = 2\pi \left(\frac{m \cos^2 \theta}{D_B(\xi)} + \frac{n \sin^2 \theta}{D_A(\xi)} \right). \quad (8)$$

Equation (8) can be treated as a more general expression of reciprocal vectors $G_{m,n}$ of QP structure, which includes arbitrary spacing nonuniform. In Eq. (8) we use two sets of parameters (d_x, d_y, θ) and (D_A, D_B, θ) to describe the CQP structure. The former one shows the origin of the structure and is convenient for analyzing in projection method, and the latter one depends directly on the real block lengths D_A and D_B , which is therefore easier to draw structure. In the rest of this paper, we use the latter form to describe the structure. The deriving using the former form will be similar.

From Eq. (8) the designing approach of the multiple-bandwidth-controlling-structure can be obtained. Specifically, if we want two arbitrary reciprocal vectors G_{m_1, n_1} and G_{m_2, n_2} to stretch with position ξ as arbitrary form $G_{m_1, n_1}(\xi)$ and $G_{m_2, n_2}(\xi)$, then resolving following equations:

$$\begin{cases} G_{m_1, n_1}(\xi) = 2\pi \left(\frac{m_1 \cos^2 \theta}{D_B(\xi)} + \frac{n_1 \sin^2 \theta}{D_A(\xi)} \right), \\ G_{m_2, n_2}(\xi) = 2\pi \left(\frac{m_2 \cos^2 \theta}{D_B(\xi)} + \frac{n_2 \sin^2 \theta}{D_A(\xi)} \right), \end{cases} \quad (9)$$

we obtain:

$$\begin{cases} D_A(\xi) = \frac{2\pi \sin^2 \theta (m_2 n_1 - m_1 n_2)}{m_2 G_{m_1, n_1}(\xi) - m_1 G_{m_2, n_2}(\xi)}, \\ D_B(\xi) = \frac{2\pi \cos^2 \theta (m_2 n_1 - m_1 n_2)}{n_1 G_{m_2, n_2}(\xi) - n_2 G_{m_1, n_1}(\xi)}. \end{cases} \quad (10)$$

Equation (10) give the form of block lengths varying with position ξ when two desired reciprocal vectors are given. As shown in Eq. (10), the two blocks vary with position as a quite complex form, which in most case is non-linear chirping.

3. Fourier transformation of CQP structure

In this section, we design a concrete CQP structure and analyze it in Fourier space. The quasi-periodic structure we choose is projected from a rectangular lattice with horizontal spacing $d_{x0} = 19.1\mu\text{m}$ and vertical spacing $d_{y0} = 17.5\mu\text{m}$ to a line with slope $\tan \theta = 0.414$, the initial block lengths are $D_{A0} = 6.69\mu\text{m}$ and $D_{B0} = 17.64\mu\text{m}$ and the lengths of positive domain in both blocks are $l = 6\mu\text{m}$. For a 10-mm-long grating, the Fourier transformation of this QP grating is:

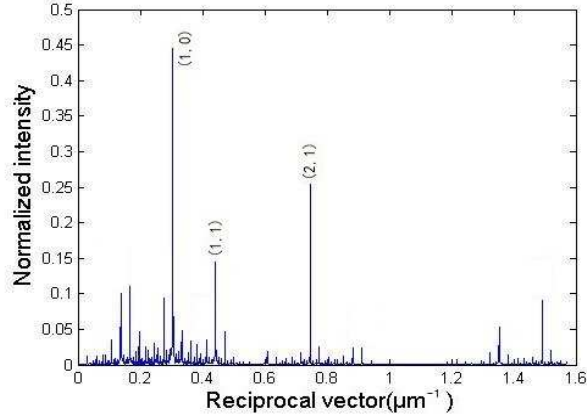


Fig. 2. Fourier transformation of a quasi-periodic grating.

Some strong reciprocal vectors are marked in Fig. 2. From Eq. (10) we know that two bandwidths can be controlled simultaneously in a CQP structure. Here we select two arbitrary reciprocal vectors, G_{11} and G_{21} , and let G_{11} holds its δ -function shape while G_{21} linearly stretches to $\pm \delta G$, the two reciprocal vectors will vary with position ζ as following forms:

$$\begin{cases} G_{1,1}(\zeta) = 2\pi \left(\frac{\cos^2 \theta}{D_{B0}} + \frac{\sin^2 \theta}{D_{A0}} \right), \\ G_{2,1}(\zeta) = 2\pi \left(\frac{2 \cos^2 \theta}{D_{B0}} + \frac{\sin^2 \theta}{D_{A0}} \right) + \frac{\zeta - L/2}{L/2} \delta G. \end{cases} \quad (11)$$

Here L is the length of the grating, ζ is the position coordinate of the grating, varies from 0 to L . Substituting (11) into (10), we obtain the relation of two block lengths vary with position:

$$\begin{cases} D_A(\zeta) = 1 / \left(\frac{1}{D_{A0}} - \frac{\delta G(\zeta - L/2)}{\pi L \sin^2 \theta} \right), \\ D_B(\zeta) = 1 / \left(\frac{1}{D_{B0}} + \frac{\delta G(\zeta - L/2)}{\pi L \cos^2 \theta} \right). \end{cases} \quad (12)$$

As expected, D_A and D_B both non-linearly vary with position ζ . From Eq. (12) we could obtain the structure parameters of the CQP grating. Here we choose $\delta G = 0.01 \mu m^{-1}$. The Fourier transformation of this structure is shown in Fig. 3 and the detail of G_{21} is shown in inset. From Fig. 3 we can see that G_{11} holds its original shape and G_{21} is stretched to $\pm 0.01 \mu m^{-1}$.

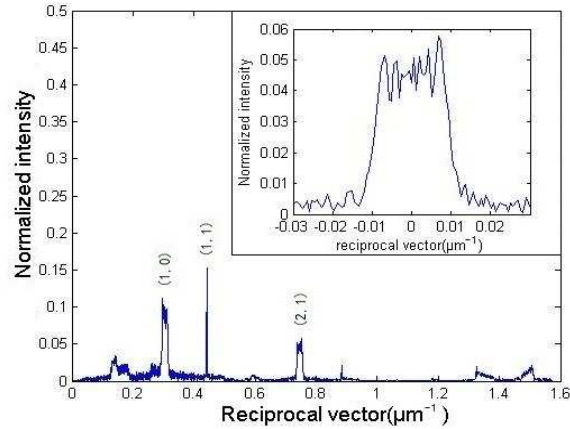


Fig. 3. Fourier transformation of the CQP grating. The inset shows the detail of G_{21} .

4. Second-harmonic generation in CQP structure

From analysis above we know that in a CQP grating some reciprocal vectors could hold the δ -function shape while the others were stretched. Thus we could expect these two kinds of reciprocal vectors will have different bandwidths in second-harmonic generation (SHG) process due to the bandwidth-broadening effect of chirped gratings [12].

We choose two reciprocal vectors of the CQP structure described in Section 3, G_{21} , which was stretched to $\pm 0.01\mu m^{-1}$, and G_{11} , which was not stretched, for numerical SHG. And we choose lithium tantalate (LT) as the nonlinear crystal and set the working temperature at $180^\circ C$. Using Sellmeier equation of LT, we can estimate that G_{11} and G_{21} can quasi-phase-match SHG process around 1334.4 and 1103.9 nm, respectively. Under the slow-varying amplitude approximation, a SHG process should satisfy the following couple-wave equations [14] during propagation:

$$\begin{cases} dE_1 / dx = -i \frac{\omega_1 d_{33} f(x)}{n_1 c} E_2 E_1^* \exp(-idkx), \\ dE_2 / dx = -\frac{i \omega_2 d_{33} f(x)}{2 n_2 c} E_1^2 \exp(idkx), \end{cases} \quad (13)$$

where E_i , ω_i , n_i indicate the electric field, angular frequency and refractive index of waves, and the subscript $i = 1, 2$ represents the fundamental and second-harmonic wave, respectively. $dk = k_2 - 2k_1$ represents the wave vector mismatch between fundamental and SH wave. Here we choose x , instead of ζ , to describe the propagating direction of waves, and $f(x)$ satisfies:

$$f(x) = \begin{cases} 1 & \text{when } x \text{ is in the positive domain,} \\ -1 & \text{when } x \text{ is in the negative domain.} \end{cases} \quad (14)$$

The numerical results of SH conversion efficiency spectrums are shown in Fig. 4. From the figure we can see, the full width at half maximum (FWHM) of the δ -function-shaped reciprocal vector G_{11} is around $0.3nm$ while the FWHM of the linearly-stretched reciprocal vector G_{21} is about $9nm$, which is 30 times that of G_{11} . The two SHG bandwidths are in good agreement with the Fourier spectrum in Fig. 3.

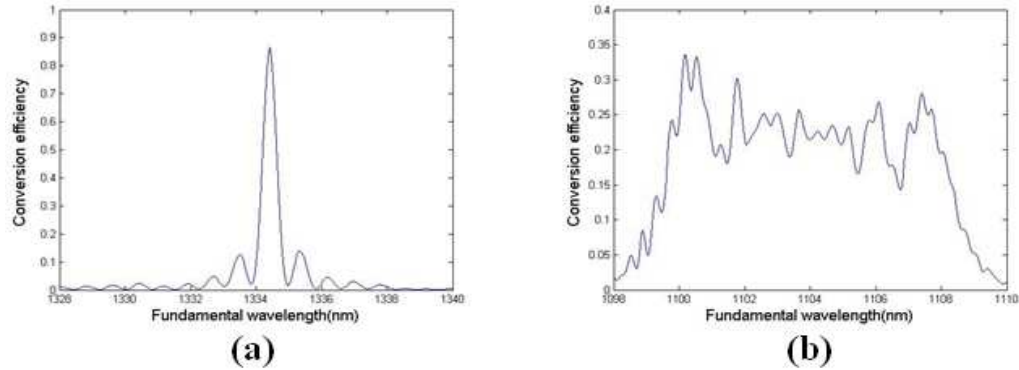


Fig. 4. SHG conversion efficiency versus fundamental wavelength using reciprocal vectors G_{11} (a) and G_{21} (b) in a CQP structure (The initial intensity of fundamental wave is $30\text{MW}/\text{cm}^2$).

Since the temperature mismatch and the wavelength mismatch can both be considered as a kind of phase-mismatch [12], based on the wavelength bandwidth data above we can obtain the temperature bandwidth of two reciprocal vectors. For the unstretched G_{11} the 0.3nm wavelength FWHM equals 2.4°C temperature FWHM, and for the stretched G_{21} the 9nm wavelength FWHM equals 134.3°C - 222.3°C , which is 88°C temperature FWHM.

The above example illustrates two bandwidths can be controlled simultaneously in a CQP grating. In cascaded processes such as THG, by designing a structure with unstretched SHG reciprocal vector and properly stretched SFG reciprocal vector (10°C for example), the two bandwidths can be overlapped with a high tolerance of temperature-shift, thus the bandwidth mismatching effect mentioned in Chapter 1 can be solved.

5. Conclusion

We have proposed a novel structure named chirped-quasi-periodic structure for both multi-QPM and bandwidth control. We have analyzed the structure in Fourier space, and performed numerical simulations of SHG in CQP. Numerical results are in good agreement with theory. For further development, the CQP structure can be used for wide-tunable visible laser source based on cascading $\chi^{(2)}$ processes, ultrashort multi-wavelength pulse-compression, et. al.

Acknowledgements:

This work was supported by the National Natural Science Foundations of China (NNSFC) under contracts 10904066 and 10874082 and the State Key Program for Basic Research of China contracts 2006CB921804 and 2010CB630703.